Basic Concepts of Rigid Fiber Suspensions Rheology

S. E. E. Hamza and A. Abu-El Hassan

Physics Department, Faculty of Science, Benha University, Benha, Egypt

www.bu.edu.eg

Abstract

In this work, fiber suspension rheology in any orthogonal system of coordinates is described in terms of the second- and fourth-order orientation tensors. At present, the theoretical basis of the dilute and semi-dilute fiber suspensions are reviewed generally. Due to the symmetry properties of the orientation tensors and normalization condition of the orientation distribution function the independent components of the second-order tensor are reduced from original "9" to "5" while the independent components of the fourth-order tensor are reduced from "81" to "13" components in any orthogonal system of coordinates. Moreover in contracted notation, these components are reduced to "3" and "5" for the second and fourth-order tensors; respectively. The closure approximation method, i.e. to approximate the even higher order tensors in terms of the lower order one; herein the fourth-order tensor in terms of the second-order tensor, is used to solve the equation of state. Various closure approximations are reviewed. Basis of some constitutive models that describe the rheological stresses in fiber suspensions are outlined. The transition from macrostructure state to the microscopic one are briefly investigated through the Folgar-Tucker as well as Advani-Tucker models. Finally, exact solutions of simple shearing flow for dilute and semi-dilute rigid fiber suspensions are performed.

Indexing terms/Keywords

Fiber suspensions, Rigid fibers, Orientation distribution function, Advani-Tucker model, Closure approximation.

Academic Discipline and Sub-Disciplines

Physics, Fluid Mechanics

SUBJECT CLASSIFICATION

Rheology of Polymers

TYPE (METHOD/APPROACH)

Theoretical Study.

INTRODUCTION

A fiber is the fundamental unit of textiles and fabrics and can be defined as a unit of matter having a length at least 100 times its width or diameter. In this range the material is said to be rigid-fibers or short-fibers. Other than these dimensions, fibers are termed as long-or flexible fibers. In industrial applications, fibers are classified into four types, namely glass fibers, carbon fibers, synthetic fibers and natural fibers. Glass and carbon fibers are added into plastic materials to reinforce the mechanical and thermal properties with negligible change in weight. The short fibers composite products are commonly manufactured by injection molding, compression molding and extrusion processes [1]. Most commercial composites contain 10% to 50% fibers by weight, which can be regarded as being concentrated suspensions. Hence, composite materials are become increasingly important due to improved physicomechanical properties. Fiber reinforced composites are of interest in many fields.

The term suspension means any solid particles suspending into a viscous or viscoelastic solvent matrix [2]. Suspensions occur in a variety of natural and man-made materials:

1. Paints – latex paints, for instance, are stable water-based emulsions of solid monomers.
2. Nano-particle suspensions, nano-fluids, are suspensions of nano-metre sized metal suspended in aqueous solvents.
3. Bacterial suspensions – the fluid mechanics of suspensions of micro-organisms is becoming an increasingly interesting topic for study. Hydrodynamic interactions in groups of microbes may play a crucial role in the formation of bio-films, since they serve as a model of non-equilibrium system.
4. Paper-pulp – the process of paper manufacture involves the processing of cellulose fiber suspensions in an aqueous medium. The orientation of fibers under flow conditions decides the property of final paper product.

Vast quantities of some of the aforementioned products are handled by the chemical, bio-chemical and pharmaceutical industries. Thus, there is a clear need for understanding the flow behavior or rheology of these systems. The difficulty in analyzing suspension flow behavior arises because suspensions are quite different of Newtonian fluids. The later, are characterized by a single material property– the shear viscosity. On the other hand, the above examples suggest that suspensions may exhibit a wide range of flow characteristics ranging from solid to gas.

Suspension rheology is more than 100 years old. Einstein's inaugural dissertation [3] can be considered as the starting point of suspension rheology. Jeffery is the pioneering one who carried out the theoretical work which the theoretical study of suspensions continued in earnest from the 1970s with a series of papers by Hinch et al. on various aspects of suspensions [4, 5, 6]. Jeffery studied theoretically the motion of an ellipsoid immersed in a simple shear Newtonian viscous flow neglecting inertia and Brownian rotation. He found that the force acting on ellipsoid reduces to two couples, one tending to make the ellipsoid adapt to the same rotation as the surrounding fluid, and the other tending to set the ellipsoid with its axes parallel to the principal axes of distortion of the surrounding fluid. In Hinch et al. work, it was found that including small Brownian motion in a fiber suspension resulted in a stationary distribution of orbits. Further researches by Hinch et al. included constitutive modeling [7, 8], characterization of fiber suspensions with Brownian motion [9, 10], and time dependent modeling [11]. Batchelor [12] provided a method of determining bulk stress from the microstructure of a fiber suspension. He also specified the conditions for the validity of ensemble and its equivalence to statistical process used often in subsequent theoretical and numerical works.

The properties of a fiber-reinforced composite are highly dependent on the orientation of the fibers. Fiber orientation affects elastic modulus, thermal expansion, and strength when the matrix is solid; viscosity when the matrix is liquid; and thermal and electrical conductivity for both solid and liquid matrices. When the composite is deformed during processing, the fibers reorient and the properties of the material change [1]. The rheological properties and fiber structure are the results of the interaction among fibers in the suspension flow. The volume fraction V_f (total volume of particles in a unit volume of suspension) and aspect ratio a_r (ratio of fiber length to diameter) are two parameters influencing the fiber structure and rheological properties of suspensions. Fiber interactions depend not only on its concentration, $V_f a_r^2$, but also on the length of fibers. Hence, on the basis of mechanical and hydrodynamic suspension interacting forces, a suspension is said to be [13, 14]:

$$\left.\begin{array}{l}\text{dilute}\\ \text{semi}-\text{dilute}\\ \text{concentrated}\end{array}\right\} \text{ if } \begin{cases} V_f a_r^2 < 1, \\ 1 < V_f a_r^2 < a_r, \\ V_f a_r^2 > a_r. \end{cases} \qquad (1)$$

The rheological properties of these fiber suspensions are classified as the following:

i. Dilute, low fiber concentration is one in which the fibers are never close to one another and do not interact [15, 16]. Therefore, each fiber can freely rotate without any hindrance from surrounding fibers with three rotational degrees of freedom.

ii. Semi-dilute or semi-concentrated, intermediate fiber concentration suspension would have no mechanical contact between the fibers, but the hydrodynamic interactions become significant. As a consequence, each fiber has two degrees of rotational freedom.

iii. Concentrated suspensions, in which the fiber orientation behavior becomes very complex [17, 18]. The average distance between two neighboring fibers is less than its diameter. Therefore, a fiber cannot rotate independently, except about its own symmetrical axis. Any motion of the fibers must involve a cooperative effort of all surrounding fibers and fiber-fiber contacts are dominate.

Usually, polymers reinforced by short fibers are molded or extruded as suspensions with the viscoelastic matrix in a liquid state. The resulting product is then cooled to make a solid composite with a given fiber orientation that is a key feature of the finished product since it affects elastic modulus, thermal and electrical conductivity, and strength of the composite material [19, 20]. Therefore, it is important to model the flow as accurately as possible in order to design and control manufacturing processes that would generate favourable fiber orientation state, which will ultimately lead to the best mechanical and thermal properties of the composite.

There are two main aspects in the research of fiber suspension flows. One aspect is to investigate the movement of fibers in flows. This research field belongs to low Reynolds number hydrodynamics. The other aspect is to investigate into the new properties of flows caused by the addition of fibers. This research field belongs to rheology. It is basically the additional stress induced by the fiber suspensions. On the other hand, there are two main ways to depict fiber orientation; the probability distribution function and the orientation tensor. Fiber suspension rheology has been investigated with different approaches; namely, experimental studies, statistical and continuum mechanics theory as well as numerical simulation studies. On this basis, Physicists, Engineers and Mathematicians has conducted in the past few decades a huge of scientific and industrial researches including dilute and semi-dilute fiber suspensions. Recently, a few theoretical works concerning concentrated fiber suspensions have been done in the last period [21].

The present article is organized as the following:

- After this introduction, the mathematical basis of the fourth-order stiffness tensor is outlined in section 2.
- Section 3 is concerned with fiber orientation description in the flow domain.
- In section 4 fiber suspension rheology are investigated.
- Some closure approximation models are reviewed in section 5.
- In section 6 constitutive equations for fiber suspensions are examined briefly.
- In section 7 examples of constitutive equations for dilute and semi-dilute fiber suspension are investigated.

- An exact solution of orientation tensor is discussed in the appendix.

REVIEW OF MATHEMATICAL BASIS

Matrix Representation and Contracted Form of the Fourth Order Tensor C_{ijkl}

For most suspensions of fibers in Newtonian and non-Newtonian fluids it is reasonable to assume that the stress tensor T_{ij} is a linear homogeny function of the deformation tensor $\dot{\gamma}_{ij}$; [22, 23]. That is; in component form:

$$T_{ij} = C_{ijkl}\,\dot{\gamma}_{kl}, \tag{2a}$$

where C_{ijkl} is the fourth-order stiffness or elasticity tensor and relation (2a) is termed as the law of elasticity. The tensor C_{ijkl} has 81 components in a matrix form. For a full anisotropic solid (i.e. 3-D random orientation), the following matrix representation can be constructed:

$$\begin{bmatrix} T_{11} \\ T_{22} \\ T_{33} \\ T_{23} \\ T_{31} \\ T_{12} \\ T_{32} \\ T_{13} \\ T_{21} \end{bmatrix} = \begin{bmatrix} C_{1111} & C_{1122} & C_{1133} & C_{1123} & C_{1131} & C_{1112} & C_{1132} & C_{1113} & C_{1121} \\ C_{2211} & C_{2222} & C_{2233} & C_{2223} & C_{2231} & C_{2212} & C_{2232} & C_{2213} & C_{2221} \\ C_{3311} & C_{3322} & C_{3333} & C_{3323} & C_{3331} & C_{3312} & C_{3332} & C_{3313} & C_{3321} \\ C_{2311} & C_{2322} & C_{2333} & C_{2323} & C_{2331} & C_{2312} & C_{2332} & C_{2313} & C_{2321} \\ C_{3111} & C_{3122} & C_{3133} & C_{3123} & C_{3131} & C_{3112} & C_{3132} & C_{3113} & C_{3121} \\ C_{1211} & C_{1222} & C_{1233} & C_{1223} & C_{1231} & C_{1212} & C_{1232} & C_{1213} & C_{1221} \\ C_{3211} & C_{3222} & C_{3233} & C_{3223} & C_{3231} & C_{3212} & C_{3232} & C_{3213} & C_{3221} \\ C_{1311} & C_{1322} & C_{1333} & C_{1323} & C_{1331} & C_{1312} & C_{1332} & C_{1313} & C_{1321} \\ C_{2111} & C_{2122} & C_{2133} & C_{2123} & C_{2131} & C_{2112} & C_{2132} & C_{2113} & C_{2121} \end{bmatrix} \begin{bmatrix} \dot{\gamma}_{11} \\ \dot{\gamma}_{22} \\ \dot{\gamma}_{33} \\ \dot{\gamma}_{23} \\ \dot{\gamma}_{31} \\ \dot{\gamma}_{12} \\ \dot{\gamma}_{32} \\ \dot{\gamma}_{13} \\ \dot{\gamma}_{21} \end{bmatrix}, \tag{2b}$$

If the fourth-order tensor C_{ijkl} demand the symmetry

$$C_{ijkl} = C_{jikl} = C_{ijlk}, \tag{3a}$$

as well as the symmetry property

$$C_{ijkl} = C_{klij}, \tag{3b}$$

then C_{ijkl} is called a completely symmetric or supper-symmetric tensor. Moreover, the symmetry of T_{ij} and $\dot{\gamma}_{ij}$ show that C_{ijkl} is symmetric not only with respect to i and j but also with respect to k and l. Thus each pair of indices in T_{ij}, C_{ijkl} and $\dot{\gamma}_{ij}$; the indices (ij) and (kl), is replaced with a single index that ranges from "1" to "6" [23, 24, 25, 26]; Table 1. Therefore, the number of components of C_{ijkl} tensor is reduced from a total of 81 to 36 independent one.

Table 1. Relationship between indices in contracted and tensor notations

Contracted notation m **or** n	**Tensor notation** ij **or** kl
1	11
2	22
3	33
4	23 or 32
5	31 or 13
6	12 or 21

As a consequence of C_{ijkl} symmetry and by using the contracted notation, it is possible to represent equation 2b in the matrix form:

$$[\sigma_i] = [C_{ij}]\,[\varepsilon_j], \tag{4a}$$

or equivalently;

$$\begin{bmatrix} \sigma_1 \\ \sigma_2 \\ \sigma_3 \\ \sigma_4 \\ \sigma_5 \\ \sigma_6 \end{bmatrix} = \begin{bmatrix} C_{11} & C_{12} & C_{13} & C_{14} & C_{15} & C_{16} \\ C_{21} & C_{22} & C_{23} & C_{24} & C_{25} & C_{26} \\ C_{31} & C_{32} & C_{33} & C_{34} & C_{35} & C_{36} \\ C_{41} & C_{42} & C_{43} & C_{44} & C_{45} & C_{46} \\ C_{51} & C_{52} & C_{53} & C_{54} & C_{55} & C_{56} \\ C_{61} & C_{62} & C_{63} & C_{64} & C_{65} & C_{66} \end{bmatrix} \begin{bmatrix} \varepsilon_1 \\ \varepsilon_2 \\ \varepsilon_3 \\ \varepsilon_4 \\ \varepsilon_5 \\ \varepsilon_6 \end{bmatrix}, \tag{4b}$$

in which the contracted notation is used to relate material property matrices σ_i, C_{ij} and ε_j to material tensors T_{ij}, C_{ijkl} and $\dot{\gamma}_{ij}$ respectively. In this notation the elements of σ_i, C_{ij} and ε_j are given by the substitution of index pairs given in Table 1. The matrix $[C]$ is known as the elastic stiffness matrix. Its elements, C_{ij}, are called the elastic constants, or the Voigt constants.

Symmetry Restrictions on Tensor Properties

If all elements of a second- and fourth-order tensor properties were independent, a very large number of separate properties would have to be measured or computed to predict the behavior of relatively simple systems. Fortunately, the tensor properties obey symmetry relations that reduce the number of independent tensorial elements. If the fourth-order tensor C_{ijkl} is symmetric, it must be satisfy the relation (3a) as well as the symmetry property given in equation 3b then C_{ijkl} is called a completely symmetric or supper-symmetric tensor. Moreover, the tensor C_{ijkl} has a maximum of 36 independent elements and can be represented by the (6×6) matrix shown in equation 4b. In addition for the symmetry property, it is usually assumed that the (6×6) contracted matrix representation of C_{ij} is symmetric with respect to its diagonal

$$C_{ij}=C_{ji};\ i,j=1,2,\ldots,6, \tag{5a}$$

then the total number of independent components is reduced from 36 to 21 (so-called Green elasticity). Thus in the most general case of well-defined anisotropic (triclinic monocrystals) the (6×6) stiffness matrix has 36 elastic constants, 21 of which can be assumed independent. Furthermore, these elements are reduced due to the symmetry to 16 elements. Moreover, due to the relation $\mathrm{tr}\,C_{ij}=1$, "tr" means the trace of a matrix or a tensor; the independent component reduced to 15 only. Hence, the final form of the stiffness matrix can be written as:

$$[C_{triclinic}]=\begin{bmatrix} C_{11} & C_{12} & C_{13} & C_{14} & C_{15} & C_{16} \\ \bullet & C_{22} & C_{23} & C_{24} & C_{25} & C_{26} \\ \bullet & \bullet & C_{33} & C_{34} & C_{35} & C_{36} \\ \bullet & \bullet & \bullet & C_{44} & C_{45} & C_{46} \\ \bullet & \bullet & \bullet & \bullet & C_{55} & C_{56} \\ \bullet & \bullet & \bullet & \bullet & \bullet & C_{66} \end{bmatrix}, \tag{5b}$$

where the matrix elements that are represented by dots are symmetric with the off-diagonal elements.

Symmetry Groups

The set of all the point symmetry operations that leave a material unchanged is called its point groups. For crystalline materials, there are 32 point groups. Most of them contain a number of different symmetry elements. Some of the results are given in Table 2, which shows the number of independent elements of second- and fourth-orders for 32 crystallographic point groups and an isotropic group. This is the number of properties that one would have to measure in order to determine the full property tensor. In section 2.2, we assume that, the Green elasticity symmetry condition, $C_{ij}=C_{ji}$, is valid for the off-diagonal elements in the stiffness matrix $[C]$. By taking Table 2 into account, the number of independent elastic constants for materials of higher symmetry (monocrystals or polycrystalline bodies) is reduced as follows:

Table 2. Basic symmetry classes and number of independent elements of tensor properties of second- and fourth-orders for 32 crystallographic point groups

Symmetry class (Bravais lattice)	Number of tensor independent coordinates	
	Second-order tensor	Fourth-order tensor
Triclinic	6	21
Monoclinic	4	13
Orthorhombic	3	9
Tetragonal	2	6
Trigonal	2	6
Hexagonal	2	5
Cubic	1	3
Isotropic	1	2

Monoclinic monocrystals (13 independent elastic constants):

$$[C_{monoclinic}] = \begin{bmatrix} C_{11} & C_{12} & C_{13} & 0 & 0 & C_{16} \\ C_{12} & C_{22} & C_{23} & 0 & 0 & C_{26} \\ C_{13} & C_{23} & C_{33} & 0 & 0 & C_{36} \\ 0 & 0 & 0 & C_{44} & C_{45} & 0 \\ 0 & 0 & 0 & C_{45} & C_{55} & 0 \\ C_{61} & C_{26} & C_{36} & 0 & 0 & C_{66} \end{bmatrix}. \quad (6a)$$

Orthorhombic monocrystals (9 independent elastic constants):

$$[C_{orthorhombic}] = \begin{bmatrix} C_{11} & C_{12} & C_{13} & 0 & 0 & 0 \\ C_{12} & C_{22} & C_{23} & 0 & 0 & 0 \\ C_{31} & C_{23} & C_{33} & 0 & 0 & 0 \\ 0 & 0 & 0 & C_{44} & 0 & 0 \\ 0 & 0 & 0 & 0 & C_{55} & 0 \\ 0 & 0 & 0 & 0 & 0 & C_{66} \end{bmatrix}. \quad (6b)$$

Tetragonal monocrystals (6 independent elastic constants):

$$[C_{tetragonal}] = \begin{bmatrix} C_{11} & C_{12} & C_{13} & 0 & 0 & 0 \\ C_{12} & C_{11} & C_{13} & 0 & 0 & 0 \\ C_{13} & C_{13} & C_{33} & 0 & 0 & 0 \\ 0 & 0 & 0 & C_{44} & 0 & 0 \\ 0 & 0 & 0 & 0 & C_{44} & 0 \\ 0 & 0 & 0 & 0 & 0 & C_{66} \end{bmatrix}. \quad (6c)$$

Trigonal monocrystals (6 independent elastic constants):

$$[C_{trigonal}] = \begin{bmatrix} C_{11} & C_{12} & C_{13} & C_{14} & 0 & 0 \\ C_{12} & C_{11} & C_{13} & -C_{14} & 0 & 0 \\ C_{13} & C_{13} & C_{33} & 0 & 0 & 0 \\ C_{14} & -C_{14} & 0 & C_{44} & 0 & 0 \\ 0 & 0 & 0 & 0 & C_{44} & C_{14} \\ 0 & 0 & 0 & 0 & C_{14} & \frac{1}{2}(C_{11}-C_{12}) \end{bmatrix}. \quad (6d)$$

Hexagonal monocrystals (5 independent elastic constants):

$$[C_{hexagonal}] = \begin{bmatrix} C_{11} & C_{12} & C_{13} & 0 & 0 & 0 \\ C_{12} & C_{11} & C_{13} & 0 & 0 & 0 \\ C_{13} & C_{13} & C_{33} & 0 & 0 & 0 \\ 0 & 0 & 0 & C_{44} & 0 & 0 \\ 0 & 0 & 0 & 0 & C_{44} & C_{14} \\ 0 & 0 & 0 & 0 & 0 & \frac{1}{2}(C_{11}-C_{12}) \end{bmatrix}. \quad (6e)$$

Cubic monocrystals (3 independent elastic constants):

$$[C_{cubic}] = \begin{bmatrix} C_{11} & C_{12} & C_{12} & 0 & 0 & 0 \\ C_{12} & C_{11} & C_{12} & 0 & 0 & 0 \\ C_{12} & C_{12} & C_{11} & 0 & 0 & 0 \\ 0 & 0 & 0 & C_{44} & 0 & 0 \\ 0 & 0 & 0 & 0 & C_{44} & 0 \\ 0 & 0 & 0 & 0 & 0 & C_{44} \end{bmatrix}. \quad (6f)$$

Isotropic materials (2 independent elastic constants):

$$\left[C_{isotropic}\right] = \begin{bmatrix} C_{12}+2C_{44} & C_{12} & C_{12} & 0 & 0 & 0 \\ C_{12} & C_{12}+2C_{44} & C_{12} & 0 & 0 & 0 \\ C_{12} & C_{12} & C_{12}+2C_{44} & 0 & 0 & 0 \\ 0 & 0 & 0 & C_{44} & 0 & 0 \\ 0 & 0 & 0 & 0 & C_{44} & 0 \\ 0 & 0 & 0 & 0 & 0 & C_{44} \end{bmatrix}. \quad (6g)$$

FIBER ORIENTATION DESCRIPTION

Moments of the Second- and Fourth-Order Tensors

The properties of fiber-reinforced composite are highly dependent on the orientation of the fibers in its flow domain [27]. The orientation of a single fiber within a continuous medium matrix can be described in spherical coordinate system by the unit vector $\underline{p}(\theta,\varphi)$ aligned along the axis of the fiber as shown in Figure 1, where θ and φ are the azimuthal and meridian angles; with $0 \le \theta \le \pi$ and $0 \le \varphi < 2\pi$, $\underline{p}$ is parallel to the major axis of an ellipsoidal particle of a single fiber with components:

$$p_1 = \sin\theta\cos\varphi;\ p_2 = \sin\theta\sin\varphi;\ p_3 = \cos\theta. \quad (7)$$

with, $p_1^2 + p_2^2 + p_3^2 = 1$.

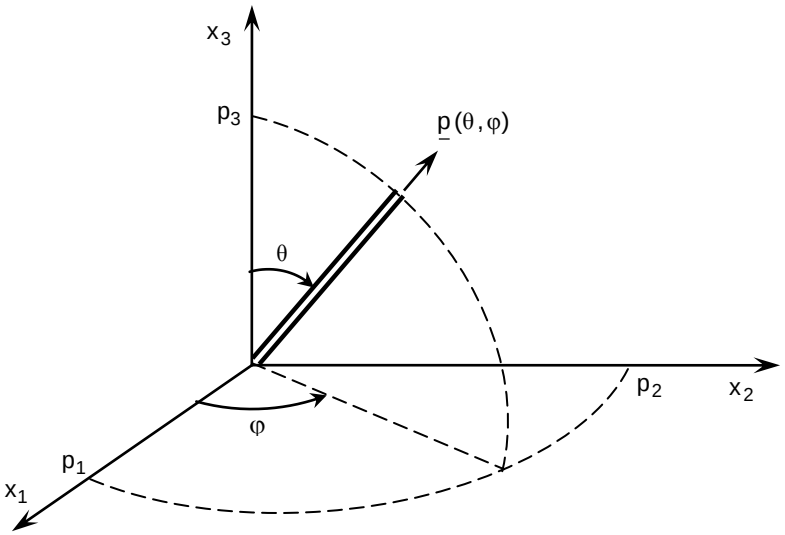

Fig 1: Orientation of a single fiber described by the unit vector $\underline{p}$ in spherical coordinates (θ, φ).

It is unrealistic attempt to develop a theory based on the orientation and motion of individual fibers, and a more useful approach is that of introducing a probability density function $\Psi(\theta,\varphi)$ whose value for a given orientation gives the probability that a fiber has particular direction. The function $\Psi(\theta,\varphi)$ defined such that the probability of a fiber oriented between the angles θ_i and $\theta_i + d\theta$ and φ_i and $\varphi_i + d\varphi$ as:

$$p(\theta_i \le \theta \le \theta_i + d\theta,\ \varphi_i \le \varphi \le \varphi_i + d\varphi) = \Psi(\theta,\varphi)\sin\theta\, d\theta\, d\varphi, \quad (8a)$$

with the normalization condition on the unit sphere,

$$\int_0^{2\pi}\int_0^{\pi} \Psi(\theta,\varphi)\sin\theta\, d\theta\, d\varphi = 1. \quad (8b)$$

The fiber distribution function is a complete description if the orientation of a single fiber is unrelated with that of any of its neighboring fibers. However, the calculations with the distribution function are too computationally cost when applied to industrially relevant flows. Therefore, the introducing of orientation tensors is a suitable way for describing the orientation state of fibers. The orientation tensors are defined as [28],

$$S_{ij} = \langle p_i p_j \rangle = \oint_{\Re^2} p_i p_j \Psi(\underline{p})\, d\Re\,, \tag{9a}$$

$$S_{ijkl} = \langle p_i p_j p_k p_l \rangle = \oint_{\Re^2} p_i p_j p_k p_l \Psi(\underline{p})\, d\Re\,. \tag{9b}$$

In general,

$$S_{ij\ldots} = \langle p_i p_j \ \ldots \ \rangle = \oint_{\Re^2} p_i p_j \ \ldots \Psi(\underline{p})\, d\Re\,, \tag{9c}$$

where $\Re^2$ is the unit sphere and the bracket "$\langle\ \rangle$" means the ensample average over a volume domain. The second-order tensor S_{ij} consists of nine components, however, due to symmetry ($S_{ij} = S_{ji}$) the components is reduced to six. These tensor components can be written as:

$$S_{ij} = \langle p_i p_j \rangle = \begin{bmatrix} \sin^2\theta\cos^2\varphi & \sin^2\theta\sin\varphi\cos\varphi & \sin\theta\cos\theta\cos\varphi \\ \bullet & \sin^2\theta\sin^2\varphi & \sin\theta\cos\theta\sin\varphi \\ \bullet & \bullet & \cos^2\theta \end{bmatrix}, \tag{9d}$$

the components of the tensor S_{ijkl} have all the information needed to describe the fiber orientation. We are left with even-ordered tensors only and all the odd are being zero due to the normalization of $\Psi(\theta,\varphi)$. For most efficient numerical simulation of the orientation state of fibers, Advani and Tucker [29] have made use of the orientation tensor which was originally introduced by Hand; [30]. The microstructure is often characterized by these second and fourth-order moments of the fiber distribution function. The normalization conditions in Equations 8b show the two fundamental symmetry properties of S_{ij}:

$$S_{ij} = S_{ji} \qquad \text{and} \qquad S_{ii} = 1. \tag{10a}$$

Similarly, any perturbation of the four subscripts keeps S_{ijkl} constant,

$$S_{iijj} = 1 \quad \text{and} \qquad S_{ijij} = 1. \tag{10b}$$

Moreover, owing to Equations 3 for the symmetry properties of S_{ijkl}; the following relations are obtained easily between the components of the two tensors S_{ij} and S_{ijkl}; namely:

$$S_{ij} = S_{ijkk}\,, \qquad S_{ij11} + S_{ij22} + S_{ij33} = S_{ij}\,, \qquad S_{ijkl} = S_{ijklpp}\,. \tag{10c}$$

Therefore, on the basis of Equation 8b the components of S_{ij} are reduced from original 9 to 5. Similarly, there are "13" independent components of S_{ijkl} [20, 31].

Although the tensors may seen an unusual means to describe fiber orientation, they have a simple physical interpretation. The main diagonal components indicate the magnitude of the fiber alignment in the direction of the reference frame, and the off-diagonal components show the rotation of principal orientation axes with respect to the coordinate system. If the fibers are randomly distributed, $\Psi = \dfrac{1}{4\pi}$, the second- and fourth-order tensors are said to be:

$$S_{ij} = \frac{1}{3}\delta_{ij}\,, \tag{11a}$$

or

$$S_{ij} = \begin{bmatrix} \frac{1}{3} & 0 & 0 \\ 0 & \frac{1}{3} & 0 \\ 0 & 0 & \frac{1}{3} \end{bmatrix}, \tag{11b}$$

where δ_{ij} is the components of the second-order identity tensor $\underline{\underline{I}}$ ($\delta_{ij} = 1, 0$ for $i = j,\ i \neq j$) and for

$$S_{ijkl} = \frac{1}{15}\left(\delta_{ij}\delta_{kl} + \delta_{ik}\delta_{jl} + \delta_{il}\delta_{jk}\right). \tag{11c}$$

Figure 2a shows isotropic orientation state, with equal orientation distribution in all directions. If all the fibers lie in the x_1x_2-plane, Figure 2b, which corresponds to planer random orientation state S_{ij} is simply:

$$S_{ij} = \begin{bmatrix} \frac{1}{2} & 0 & 0 \\ 0 & \frac{1}{2} & 0 \\ 0 & 0 & 0 \end{bmatrix}. \quad (11d)$$

For perfectly aligned orientation in x_1-direction, Figure 2c, S_{ij} is written as:

$$S_{ij} = \begin{bmatrix} 1 & 0 & 0 \\ 0 & 0 & 0 \\ 0 & 0 & 0 \end{bmatrix}. \quad (11e)$$

We can then observe that, the orientation tensor S_{ij} is symmetric and has a unit trace ($trS_{ij} = 1$) due to the unit length of $\underline{p}$ and the normalization condition. For a completely random orientation state $S_{ij} = \frac{1}{3}\delta_{ij}$ and the limit that all the fibers are perfectly aligned in the x_1-direction the only nonzero component of S_{ij} is $S_{11} = 1$. We limit our discussion to the second-order and the fourth-order tensors because they are rheologically sufficient.

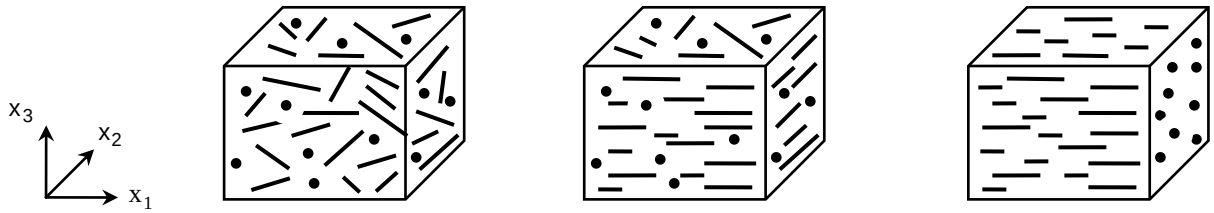

(a) 3-D random (b) planer random (c) aligned

Fig 2: Example of different orientation states.

The Matrix Representation in Six Dimensional Space

As will be indicated in the following subsections, the fiber orientation distribution can be visualized by using eigenvalues I, II and III and eigenvectors $\hat{e}_i$ $(i = 1,2,3)$ of the second-order orientation tensor $\underline{\underline{S}}_2$; Figure 3. The eigenvectors indicate the principal directions of fiber aligned and the eigenvalues give the statistical proportions (0 to 1) of fibers aligned with respect to those directions $\hat{e}_i$ $(i = I, II, III)$.

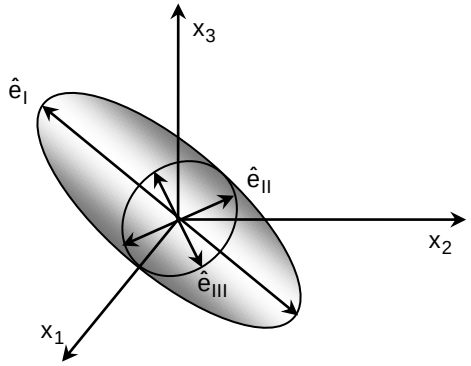

Fig 3: Schematic representation of orientation distribution by the second-order orientation tensor.

If the stress and the rate of strain deformation second-order tensors t_{ij} and $\dot{\gamma}_{ij}$ has t_i and e_i components where t_i and e_i are the principal stresses and strains, then in the six-dimensional space the following representation can be observed [32].

$$\begin{pmatrix} t_I \\ t_{II} \\ t_{III} \\ 0 \\ 0 \\ 0 \end{pmatrix} = \begin{pmatrix} C_{11} & C_{12} & C_{13} & C_{14} & C_{15} & C_{16} \\ C_{12} & C_{22} & C_{23} & C_{24} & C_{25} & C_{26} \\ C_{13} & C_{23} & C_{33} & C_{34} & C_{35} & C_{36} \\ C_{14} & C_{24} & C_{34} & C_{44} & C_{45} & C_{46} \\ C_{15} & C_{25} & C_{35} & C_{45} & C_{55} & C_{56} \\ C_{16} & C_{26} & C_{36} & C_{46} & C_{56} & C_{66} \end{pmatrix} \begin{pmatrix} e_I \\ e_{II} \\ e_{III} \\ 0 \\ 0 \\ 0 \end{pmatrix}. \quad (12a)$$

The last equation, in shorthand form, can be rewritten as:

$$\begin{pmatrix} t_{princ} \\ 0 \end{pmatrix} = \begin{pmatrix} C_{AA} & C_{AB} \\ C_{BA} & C_{BB} \end{pmatrix} \begin{pmatrix} e_{princ} \\ 0 \end{pmatrix}, \quad (12b)$$

with $A = 1,2,3$ and $B = 4,5,6$

FIBER SUSPENSION RHEOLOGY

A comprehensive treatment of fiber suspension flow in complex geometries involves flow-orientation coupling is investigated [33]. It is well understood that fibers orient in response to flow kinematics, while the suspension rheology is defined in the concentration and orientation of the suspended fiber. Flow simulations that incorporate flow-orientation coupling further emphasize the need for including these fully coupled evaluations to make accurate predictions in certain geometries.

Jeffery's Model

Jeffery's model of fiber suspension requires uninteracting fibers, and hence it is thus valid in the dilute and partially-dilute regimes only. Most typical industrial applications are in the concentrated regime, and as such the Jeffery's model is clearly not sufficient for industrial use. The motion of a single fiber in a Newtonian flow can be described by Jeffery's model under the following assumptions [31]: (1) the fiber may be represented by an ellipsoid of revolution; (2) no-slip conditions prevail at the surface of the fiber; (3) the velocity field is only locally perturbed by the motion of the fiber; (4) there is no interaction between fibers; (5) the flow far from the fiber is steady and homogeneous on a length scale that is large compared to the fiber dimensions; (6) the motion is sufficiently slow that inertia forces are negligible; (7) the fiber translates with the fluid velocity as a function of location through the part thickness. Jeffery's model in its vector form and index notation is written as:

$$\frac{D\underline{p}}{Dt} = \dot{\underline{p}} = -\underline{\underline{\omega}} \cdot \underline{p} + \alpha\left(\underline{\underline{\dot{\gamma}}} \cdot \underline{p} - \dot{\gamma} : \underline{ppp}\right), \tag{13a}$$

$$\frac{Dp_i}{Dt} = \dot{p}_i = -\omega_{ij} p_j + \alpha\left(\dot{\gamma}_{ij} p_j - \dot{\gamma}_{kl} p_k p_l p_i\right), \tag{13b}$$

where α is a constant defining the ellipticity of the particle and termed as the shape factor of the fiber, it depends on the fiber aspect ratio a_r as:

$$\alpha = \frac{a_r^2 - 1}{a_r^2 + 1}, \tag{13c}$$

for slender fibers $\alpha \to 1$. In equations 13a, $D/Dt = \partial/\partial t + \left(\underline{v} \cdot \nabla\right)$ is the material time derivative, $\underline{\underline{\dot{\gamma}}} = \frac{1}{2}\left[\nabla \underline{v} + (\nabla \underline{v})^T\right]$ is the deformation (stretching) tensor and $\underline{\underline{\omega}} = \frac{1}{2}\left[\nabla \underline{v} - (\nabla \underline{v})^T\right]$ is the vorticity (spin) tensor.

Equation of Continuity (Fokker-Planck Equation)

For dilute suspensions, the kinetics of orientation distribution function Ψ is governed by the equation of continuity for Ψ or the so called Fokker-Planck equation [29]; namely,

$$\frac{D\Psi}{Dt} = -\nabla_p \cdot \left(\dot{\underline{p}}\Psi\right), \tag{14}$$

where ∇_p is the surface gradient operator in orientation space and $\left(\dot{\underline{p}}\Psi\right)$ is the flux probability. To solve Equation 14 for Ψ, a constitutive relation for the time rate of change of the fiber orientation vector $\dot{\underline{p}}$ is needed.

Equations of Motion for S_{ij} and S_{ijkl}

Instead of performing the integration and tedious calculation of the distribution function, an equivalent system of differential equations can be written that characterizes the orientation evaluation in terms of the tensors S_{ij} and S_{ijhl}. Consider the second-order tensor $B_{ij}(\underline{p}) = p_i p_j$ for $i, j \in \{1, 2, 3\}$ is related to the second-order orientation tensor, S_{ij}, through integration as:

$$\oint_{\Re^2} \Psi B_{ij}\, d\Re = \oint_{\Re^2} \Psi p_i p_j\, d\Re = S_{ij}, \tag{15a}$$

multiply the equation of continuity in Equation 14 with B_{ij}

$$\frac{D\Psi}{Dt} B_{ij} = -\nabla_p \cdot \left(\dot{\underline{p}}\Psi\right) B_{ij}, \tag{15b}$$

and performing integration over the unit sphere $\Re^2$;

$$\therefore \quad \oint_{\Re^2} \frac{D\Psi}{Dt} B_{ij} d\Re = -\oint_{\Re^2} \nabla_p \cdot \left(\dot{\underline{p}}\Psi\right) B_{ij} d\Re \,, \tag{15c}$$

the left hand side of Equation 15c is desired from the equation of motion for the second-order orientation tensor S_{ij} which is seen to be:

$$\oint_{\Re^2} \frac{D\Psi}{Dt} B_{ij} d\Re = \frac{D}{Dt} \oint_{\Re^2} \Psi B_{ij} d\Re = \frac{D}{Dt} \oint_{\Re^2} \Psi p_i p_j d\Re = \frac{DS_{ij}}{Dt} \,. \tag{16a}$$

The chain rule may be used to expand the right hand side of Equation 16a. Therefore, the equation of motion for the second-order orientation tensor becomes:

$$\frac{DS_{ij}}{Dt} = \oint_{\Re^2} \dot{p}\Psi \cdot \left(p_i p_j\right) d\Re \,, \tag{16b}$$

the right-hand side is the rate of change of motion due to hydrodynamic forces, which is essentially the same as given by Jeffery's equation. By using the chain rule, we can rewrite the right-hand side of Equation 16b in the following form:

$$\oint_{\Re^2} \dot{p}\Psi \cdot \left(p_i p_j\right) d\Re = -\left(\omega_{ik} S_{kj} - S_{ik}\omega_{kj}\right) + \alpha\left(\dot{\gamma}_{ik} S_{kj} + S_{ik}\dot{\gamma}_{kj} - 2\dot{\gamma}_{kl} S_{ijkl}\right). \tag{16c}$$

Therefore, the equation of motion for the second-order orientation tensor S_{ij} is obtained by combining Equations 15b and 16c to obtain:

$$\frac{DS_{ij}}{Dt} = -\left(\omega_{ik} S_{kj} - S_{ik}\omega_{kj}\right) + \alpha\left(\dot{\gamma}_{ik} S_{kj} + S_{ik}\dot{\gamma}_{kj} - 2\dot{\gamma}_{kl} S_{ijkl}\right), \tag{17a}$$

or

$$\dot{\underline{\underline{S}}}_2 = \frac{D\underline{\underline{S}}_2}{Dt} = -\left(\underline{\underline{\omega}} \cdot \underline{\underline{S}}_2 - \underline{\underline{S}}_2 \cdot \underline{\underline{\omega}}\right) + \alpha\left(\dot{\underline{\underline{\gamma}}} \cdot \underline{\underline{S}}_2 + \underline{\underline{S}}_2 \cdot \dot{\underline{\underline{\gamma}}} - 2\dot{\underline{\underline{\gamma}}} : \underline{\underline{S}}_4\right). \tag{17b}$$

In the same manner, the equation of motion for the fourth-order orientation tensor S_{ijhl} is given as:

$$\begin{aligned} \frac{DS_{ijkl}}{Dt} = &-\left(\omega_{im} S_{mjkl} - S_{ijkm}\omega_{ml} + \omega_{jm} S_{iklm} - S_{ijlm}\omega_{mk}\right) \\ &+ \alpha\left(\dot{\gamma}_{im} S_{jklm} + \dot{\gamma}_{jm} S_{iklm} + \dot{\gamma}_{km} S_{ijlm} + \dot{\gamma}_{lm} S_{ijkm} - 2\dot{\gamma}_{mn} S_{ijklmn}\right) \end{aligned} \tag{17c}$$

or

$$\dot{\underline{\underline{S}}}_4 = \frac{D\underline{\underline{S}}_4}{Dt} = \frac{1}{2}\left(\underline{\underline{\omega}} \cdot \underline{\underline{S}}_4 - \underline{\underline{S}}_4 \cdot \underline{\underline{\omega}}\right) + \frac{\alpha}{2}\left(\dot{\underline{\underline{\gamma}}} \cdot \underline{\underline{S}}_4 + \underline{\underline{S}}_4 \cdot \dot{\underline{\underline{\gamma}}} - 2\dot{\underline{\underline{\gamma}}} : \underline{\underline{S}}_6\right), \tag{17d}$$

Effect of Interaction among Fibers

Modeling the interactions between two fibers in a fluid suspension is difficult. It is assumed that fiber interactions are due to volume averaged effects. The model for fiber interactions is similar to the theory of rotary Brownian motion where ellipsoids experience small forces as they collide within the suspension causing torques on each ellipsoid. To take into account the fiber interaction effects in semi-concentrated suspensions, Folgar and Tucker [34] proposed the inclusion interaction of a diffusion term, a flux vector $\underline{q}$ through Equation 14 i.e.,

$$\frac{D\Psi}{Dt} = -\nabla_p \cdot \left(\dot{\underline{p}}\Psi + \underline{q}\right), \tag{18}$$

with the increase of suspension concentration, fiber-fiber contacts also increase, causing deviations from the orientation state observed in dilute suspensions. The diffusive flux vector $\underline{q}$ represents a phenomenological way to account for these deviations. In order to model the diffusive flux vector in Equation 18, Folgar and Tucker suggested the relationship:

$$\underline{q} = -\nabla\left(D_r \Psi\right), \tag{19}$$

where D_r is the rotary diffusivity. At present, it is sufficient to assume that D_r may be a function of (θ, φ) and as such cannot be brought out of the gradient operator. When the assumption of Folgar-Tucker is taken into consideration, the flow of fiber is given by the equation of continuity:

$$\begin{aligned}\frac{D\Psi}{Dt} &= -\nabla_p \cdot \left[\dot{\underline{p}}\Psi - \nabla_p\left(D_r \Psi\right)\right] \\ &= -\nabla_p \cdot \left[\dot{\underline{p}}\Psi\right] + \nabla_p^2\left[D_r \Psi\right].\end{aligned} \tag{20}$$

where ∇_p^2 represents the Laplacian operator on the orientation space. In case of Jeffery's model, no fiber interaction occurs and hence the rotary diffusion expression $D_r = 0$.

By the same method given in section (4.3), the equation of motion for S_{ij} with introducing the diffusion term, is given by:

$$\frac{DS_{ij}}{Dt} = -\left(\omega_{ik}S_{kj} - S_{ik}\omega_{kj}\right) + \alpha\left(\dot{\gamma}_{ik}S_{kj} + S_{ik}\dot{\gamma}_{kj} - 2\dot{\gamma}_{kl}S_{ijkl}\right) + 2D_r\left(\delta_{ij} - 3S_{ij}\right), \tag{21a}$$

or equivalently

$$\frac{D\underline{\underline{S}}_2}{Dt} = \underbrace{-\left(\underline{\underline{\omega}}\cdot\underline{\underline{S}}_2 - \underline{\underline{S}}_2\cdot\underline{\underline{\omega}}\right) + \alpha\left(\underline{\underline{\dot{\gamma}}}\cdot\underline{\underline{S}}_2 + \underline{\underline{S}}_2\cdot\underline{\underline{\dot{\gamma}}} - 2\underline{\underline{\dot{\gamma}}}:\underline{\underline{S}}_4\right)}_{\text{hydrodynamic contribution}} + \underbrace{2D_r\left(\underline{\underline{I}} - 3\underline{\underline{S}}_2\right)}_{\text{Diffusive contribution}}. \tag{21b}$$

In the same manner, the equation of motion of the fourth-order tensor S_{ijkl} is:

$$\begin{aligned}\frac{DS_{ijkl}}{Dt} = &-\left(\omega_{im}S_{mjkl} - S_{ijkm}\omega_{ml} + \omega_{jm}S_{iklm} - S_{ijlm}\omega_{mk}\right) \\ &+ \alpha\left(\dot{\gamma}_{im}S_{jklm} + \dot{\gamma}_{km}S_{iklm} + \dot{\gamma}_{km}S_{ijlm} + \dot{\gamma}_{lm}S_{ijkl} - 2\dot{\gamma}_{mn}S_{ijklmn}\right) \\ &+ 2D_r\left[-10S_{ijkl} + S_{ij}\delta_{kl} + S_{ik}\delta_{jl} + S_{il}\delta_{jk} + S_{jk}\delta_{il} + S_{jl}\delta_{ik} + S_{kl}\delta_{ij}\right].\end{aligned} \tag{21c}$$

The evaluation of the second-order orientation tensor requires knowledge of the fourth-order orientation tensor S_{ijkl}, which induces the classic closure problem. The time required to compute the evaluation of the second-order orientation tensor S_{ij} is significantly less than the computational time required to evolve $\Psi(\underline{p})$ once an approximate method is selected to approximate the fourth-order orientation tensor S_{ijkl}.

More about the Constant D_r

For three decades, approaches to model fiber orientation while incorporating fiber interaction effects, are based on Folgar-Tucker model [34]. Their model introduces interaction between fibers through forces similar to Brownian motion. For non-dilute suspensions, Folgar and Tucker hypothesized that fiber interaction acted similarly to isotropic diffusion and a result added diffusion like term to Jeffery's equation. They proposed a diffusivity function based on the rate of deformation tensor $\underline{\underline{\dot{\gamma}}}$ and an empirically derived parameter C_I termed as the interaction coefficient; defined as:

$$D_r = C_I\left\|\underline{\underline{\dot{\gamma}}}\right\|, \tag{22a}$$

where C_I is assumed to be a function of volume fraction V_f (a large C_I implies more fiber-fiber interactions) and $\left\|\underline{\underline{\dot{\gamma}}}\right\|$ is the scalar magnitude of the rate of deformation tensor; $\left\|\underline{\underline{\dot{\gamma}}}\right\| = \sqrt{\frac{1}{2}\left(\underline{\underline{\dot{\gamma}}} : \underline{\underline{\dot{\gamma}}}\right)}$ with $\underline{\underline{\dot{\gamma}}} : \underline{\underline{\dot{\gamma}}} = \dot{\gamma}_{ij}\dot{\gamma}_{ji}$.

By assuming the diffusivity term is of the form given by Folgar and Tucker, Equation 21a, and using Equation 22a the resulting equation of motion of the second-order orientation tensor is written as:

$$\frac{DS_{ij}}{Dt} = -\left(\omega_{ik}S_{kj} - S_{ik}\omega_{kj}\right) + \alpha\left(\dot{\gamma}_{ik}S_{kj} + S_{ik}\dot{\gamma}_{kj} - 2\dot{\gamma}_{kl}S_{ijkl}\right) + 2C_I\left\|\dot{\gamma}_{ij}\right\|\left(\delta_{ij} - 3S_{ij}\right), \tag{22b}$$

the particle shape factor is very close to unity due to the large length-to-radius ratio of fibers; i.e. slender model. This model yields exceptional results compared to previous theories, and has been considered the standard throughout both the industrial and academic communities. The Folgar and Tucker model is considered to be the benchmark for fiber orientation analysis during processing and has found wide acceptance in the literature. The empirically determined interaction coefficient C_I ensures that the final orientation state is accurately captured.

The Folgar-Tucker model allows for the control of the steady state fiber orientation through the magnitude of C_I but the rate of fiber reorientation is still dominated by the flow field for typical values of C_I. Small values (16×10^{-4} to 1×10^{-4}) [29] typically provide a good fit to experimental fiber orientation data. Bay [35] developed an empirical expression for concentrated suspensions ($V_f > a_r^{-1}$),

$$C_I = 0.0184 \exp(-0.7148\, V_f\, a_r)\,. \tag{23a}$$

Equation 23a predicts that C_I decreases for increasing $V_f\, a_r$, a result explained by a proposed caging effect.

Phan-Thien et al. (2002) [36] proposed a model in which C_I increases with increasing $V_f\, a_r$ as:

$$C_I = M\left[1 - \exp\left(-NV_f\, a_r\right)\right]\,, \tag{23b}$$

where M and N are constants. Phan-Thien et al. [36] determined $M = 0.03$ and $N = 0.224$ by fitting Equation 23b to experimental data in comparison with Folgar and Tucker model for various suspensions of nylon fibers subject to simple shear flow. Recently, the parameter proposed by Sepehr et al. (2004a); [37], can be incorporated into the Folgar-Tucker model as follows:

$$\frac{DS_{ij}}{Dt} = \alpha\left[\left(\omega_{ik}S_{kj} - S_{ik}\omega_{kj}\right) + \left(\dot{\gamma}_{ik}S_{kj} + S_{ik}\dot{\gamma}_{kj} - 2\dot{\gamma}_{kl}S_{ijkl}\right) + 2C_I\left\|\dot{\gamma}_{ij}\right\|\left(\delta_{ij} - 3S_{ij}\right)\right]. \tag{23c}$$

To solve Equations 22b and 23c closure approximation approach is needed to express the fourth-order tensor S_{ijkl} in terms of the second-order tensor S_{ij}.

CLOSURE APPROXIMATION

The evolution equation of any orientation tensor contains next higher even-order tensor; say S_{ij} in Equation 20a contains S_{ijkl} and S_{ijkl} in Equation 20c contains S_{ijklmn} and so on. Thus, one needs a closure approximation to close the set of the evolution equations of the orientation tensors. A fourth-order closure may be expressed as:

$$S_{ijkl} \approx F_{ijkl}(S_{mn})\,, \tag{24}$$

where F_{ijkl} is a function of the second-order tensor S_{mn}. There have been many methods proposed to address the closure problem.

Most types of closure approximations are Linear (L), quadratic (Q) and a Hybrid (H) which is being a combination of (L) and (Q) closure approximations. One of the popular models used in the numerical simulation of real manufacturing processes, such as injection molding, compression molding, is the (H) closure approximation [29, 38, 39] since it shows stable behavior of fiber orientation state with reasonable computational efficiency.

A Hybrid closure approximation has readily been used for its stable behaviors in spite of its over prediction of orientation components compared with distribution function approximation. Cintra and Tucker [26] developed orthotropic fitted closure approximation by assuming that the principal directions of the fourth-order orientation tensor S_{ijkl} are functions of the eigenvalues of the second-order orientation tensor S_{ij}. Known parameters where determined by fitting selected flow data obtained from probability distribution function.

Orthotropic closure approximation shows better behaviors than previous closure approximation but unfortunately suffers from non-physical oscillations at low value of fiber-fiber interaction coefficient C_I. Chung and Kwon [40] have proposed Orthotropic closure approximation [41] which overcome such problems of non-physical oscillations. However, such orthotropic type closure approximation require additional computation time for the transformation between the global coordinate system and the principal coordinate system. In this respect, Chung and Kwon [42] have proposed invariant based optimal fitting closure approximation, which significantly reduces the computation time. Finally; equation of the hybrid closure approximation which is a combination of linear and quadratic closure approximations as well as other closure approximations are, summarized by the following equations:

Linear Closure Approximation (L)

An even simpler closure approximation is the linear one which originally introduced by Hand [43]:

$$S^L_{ijkl} = \frac{-1}{35}\left(\delta_{ij}\delta_{kl} + \delta_{ik}\delta_{jl} + \delta_{il}\delta_{jk}\right) + \frac{1}{7}\left(S_{ij}\delta_{kl} + S_{ik}\delta_{jl} + S_{il}\delta_{jk} + S_{kl}\delta_{ij} + S_{jl}\delta_{ik} + S_{jk}\delta_{il}\right). \tag{25a}$$

In general form:

$$S^L_{ijkl} = \frac{-1}{(4+N_L)(2+N_L)}\left(\delta_{ij}\delta_{kl} + \delta_{ik}\delta_{jl} + \delta_{il}\delta_{jk}\right) + \frac{1}{(4+N_L)}\left(S_{ij}\delta_{kl} + S_{ik}\delta_{jl} + S_{il}\delta_{jk} + S_{kl}\delta_{ij} + S_{jl}\delta_{ik} + S_{jk}\delta_{il}\right), \tag{25b}$$

where N_L refers to a space dimensions; i.e.,

$$N_L = \begin{cases} 2 & \text{in } 2D, \\ 3 & \text{in } 3D. \end{cases} \tag{25c}$$

This closure approximation is exact for a random distribution of fiber orientations (an isotropic suspension). Also, it is exact for a completely isotropic distribution of fiber orientations,

$$S^{L}_{ijkl} = S_{ij}S_{kl}\,, \tag{25d}$$

which is exact for aligned fibers.

Quadratic Closure Approximation (Q)

This closure is exact (and not approximation) for perfectly aligned fibers;

$$S^{Q}_{ijkl} = S_{ij}S_{kl}\,. \tag{26a}$$

Although the quadratic closure is frequently used with an other closures, it does not obey the symmetry requirements for a fourth-order orientation tensor, i.e.

$$S^{Q}_{ijkl} \neq S^{Q}_{klij} \qquad \forall \;\; i, j, k, l\,. \tag{26b}$$

Hybrid Closure Approximation (H)

The hybrid closure proposed by Advani and Tucker [29] is the most widely used method in industry because of its algebraic simplicity and numerical robustness. As we have seen in the last two subsections, the linear closure approximation is exact for random distribution of orientation while the quadratic one is exact for highly aligned fibers. The hybrid closure approximations have proposed to improve the accuracy for the intermediate cases of fiber orientations and still remain exact at two limits. It is a linear combination between the quadratic closure and the linear closure as:

$$S^{H}_{ijkl} = (1-f)\,S^{L}_{ijkl} + f\,S^{Q}_{ijkl}\,, \tag{27a}$$

where "f" represents the scalar measure of orientation (weighting function) with,

$$f = 1 - N_H \det\left(S_{ij}\right), \tag{27b}$$

and

$$N_H = \begin{cases} 4 & \text{in } \; 2D, \\ 27 & \text{in } \; 3D. \end{cases}. \tag{27c}$$

Two expressions for the weighting function "f " in terms of the tensor S_{ij} have been suggested by Advani and Tucker [29], such that "$f = 1$" for perfectly aligned fibers (as one expects in steady uniaxial extension) and "$f = 0$" for completely random distribution of fiber orientations (an isotropic suspension):

Natural Closure Approximation (N)

The natural closure approximation [44] is formed through the fitting process of the general expression of a fully symmetric S_{ijkl} in terms of S_{ij}. This type of closure in two dimensional case takes the form:

$$S^{N}_{ijkl} = \frac{1}{6}\left[\det(S_{ij})\right]\left(\delta_{ij}\delta_{kl} + \delta_{ik}\delta_{jl} + \delta_{il}\delta_{jk}\right) + \frac{1}{3}\left(S_{ij}\delta_{kl} + S_{ik}\delta_{jl} + S_{il}\delta_{jk}\right), \tag{28}$$

Invariant Based Optimal Fitting Closure Approximation (IBOF)

This closure starts with the most general expression of the fourth-order tensor S_{ijkl} in terms of the two second-order tensors S_{ij} and δ_{ij} as follows [42]:

$$S_{ijkl} = \beta_1 F\left(\delta_{ij}\delta_{kl}\right) + \beta_2 F\left(\delta_{ij}S_{kl}\right) + \beta_3 F\left(S_{ij}S_{kl}\right) + \beta_4 F\left(\delta_{ij}S_{km}S_{ml}\right) + \beta_5 F\left(S_{ij}S_{km}S_{ml}\right) + \beta_6 F\left(S_{im}S_{mj}S_{kn}S_{nl}\right), \tag{29a}$$

where the operator "F" indicates the symmetric part of the argument for instance; i.e.,

$$\begin{aligned} F(T_{ijkl}) = \frac{1}{24}\big(&T_{ijkl} + T_{jikl} + T_{ijlk} + T_{jilk} + T_{klij} + T_{lkij} + T_{kjli} + T_{lkji} + T_{ikjl} + T_{kjil} + T_{iklj} + T_{kilj} \\ &+ T_{jlik} + T_{ljik} + T_{jlki} + T_{ljki} + T_{iljk} + T_{lijk} + T_{ilkj} + T_{likj} + T_{jkil} + T_{kjil} + T_{jkli} + T_{kjli}\big). \end{aligned} \tag{29b}$$

Invariant based closure assumes that the coefficients $\beta_1 \to \beta_6$ are polynomial expansions of the second and third invariants of S_{ij}; i.e., II and III. It can be easily shown that, among the six β_i's in equation 29a, there are only three independent values with the rest being determined in terms of the three independent ones with the help of the normalization conditions and full symmetry between indices together with Cayley-Hamilton theorem.

The Neural-Network-Based Optimal Fitting Closure Approximation (NNBOF)

This closure approximation was developed recently by Jack et al. [44] . It assumes two-layer neural-network between the second and fourth-order orientation tensors $\underline{\underline{S}}_2$ and $\underline{\underline{S}}_4$ as follows;

$$\tilde{\underline{\underline{S}}}_4 = f_2\left[\Omega_2 \cdot f_1\left(\Omega_1 \cdot \tilde{\underline{\underline{S}}}_2 + b_1\right) + b_2\right] , \tag{30}$$

where $\tilde{\underline{\underline{S}}}_4$ and $\tilde{\underline{\underline{S}}}_2$ are, respectively the independent values of $\underline{\underline{S}}_4$ and $\underline{\underline{S}}_2$, Ω_i $(i=1, 2)$ are the net-work weights, b_i are the net-work bases and f_i are respectively the hyperbolic tangent transfer function and the pure linear transformation function. The neural-network closure approximation is accurate for a wide range of the flow fluids, and also its computational time is much lower than the orthotropic closures.

CONSTITUTIVE EQUATION FOR FIBER SUSPENSIONS

There are two ways to construct the constitutive equations for fiber suspensions: the continuum mechanics approach and microstructure modeling. Several constitutive models have been proposed to describe the stress tensor for a suspension of particles in a Newtonian fluid. The constitutive equations for such systems, either obtained by invoking continuum mechanics or by using microstructure information, have the same form despite different starting points. In general, the total viscous stress tensor for the suspension, τ_{ij}, is taken to be the sum of the stress contributions from the Newtonian suspending fluid, τ_{ij}^n, and from the fiber, τ_{ij}^f. Hence, the resulting constitutive equations for the suspension can be expressed as:

$$\tau_{ij} = \tau_{ij}^n + \tau_{ij}^f , \tag{31a}$$

$$\tau_{ij}^n = -P\delta_{ij} + \mu_o \dot{\gamma}_{ij} , \tag{31b}$$

where μ_o is the solvent (dynamical) viscosity and P is the hydrostatic pressure. To model the fiber stress tensor, Advani and Tucker [29] assume that:

$$\underline{\underline{\tau}}^f = \mu_o V_f \left[\mu_1 \dot{\underline{\underline{\gamma}}} : \underline{\underline{S}}_4 + \mu_2\left(\dot{\underline{\underline{\gamma}}} : \underline{\underline{S}}_2 + \underline{\underline{S}}_2 : \dot{\underline{\underline{\gamma}}}\right) + \mu_3 \dot{\underline{\underline{\gamma}}} + 2\mu_4 D_r \underline{\underline{S}}_2\right] , \tag{32a}$$

or, in component form,

$$\tau_{ij}^f = \mu_o V_f \left[\mu_1 \dot{\gamma}_{kl} S_{ijkl} + \mu_2\left(\dot{\gamma}_{ik} S_{kj} + S_{ik}\dot{\gamma}_{kj}\right) + \mu_3 \dot{\gamma}_{ij} + 2\mu_4 D_r S_{ij}\right], \tag{32b}$$

μ_i $(i=1, 2, 3, 4)$ are positive material parameters specified by the particle aspect ratio, a_r. The term involving D_r accounts for Brownian motion. Most constitutive models for dilute and semi-dilute suspensions differ from each other based on how the material parameters μ_i are defined. The explicit expressions for μ_i suggested by different constitutive models have been discussed and reviewed [9, 31, 45]. Examples of these parameters are shown in Table 3.

Table 3. Explicit expressions for μ_i suggested by different constitutive models.

Models	Material Parameters
Hinch et al. (1972)	$\mu_1 = 2, \quad \mu_2 = \frac{a_r^2}{2[\ln(2a_r) - 1.5]}, \quad \mu_3 = \frac{6\ln 2a_r - 11}{a_r^2}, \quad \mu_4 = 0$
Lipscomb et al. (1988)	$\mu_1 = 2, \quad \mu_2 = \frac{a_r^2}{2\ln a_r}, \quad \mu_3 = \mu_4 = 0$
Shaqfeh et al. (1990)	$\mu_2 = -\frac{16a_r^3}{3\ln V_f}\left[1 + \frac{\ln(-\ln V_f)}{\ln V_f} - \frac{0.6634}{\ln V_f}\right], \quad \mu_1 = \mu_3 = \mu_4 = 0.$

For a slender particle, particle thickness can be ignored producing μ_2 and μ_3 equal to zero. If the particle is large enough so that Brownian motion can be ignored, last term containing D_r can be omitted. Therefore, typical fiber stress tensor for dilute suspensions can be expressed as follows:

$$\tau_{ij}^f = \mu_o \mu_1 V_f \, \dot{\gamma}_{kl} S_{ijkl} , \tag{33a}$$

and

$$\mu_1 = \frac{a_r^2}{\left(\ln 2a_r - \frac{3}{2}\right)} \approx \frac{a_r^2}{\ln a_r}, \tag{33b}$$

In semi-dilute suspensions a hydrodynamic interaction between the particles exists. For such material systems, an expression similar to equation 33a was proposed by Dinh and Armstrong [46] as:

$$\tau_{ij}^f = \mu_o \frac{\pi n \ell^3}{6 \ln(2h/d)} \dot{\gamma}_{kl} S_{ijkl}, \tag{34a}$$

where "n" is the fiber number density, "ℓ" and "d" are the length and diameter of the fiber and "h" is defined to be the average fiber spacing as:

$$h = \begin{cases} (n\ell)^{-1/2} & \text{for aligned orientations,} \\ (n\ell^2)^{-1} & \text{for random orientations.} \end{cases} \tag{34b}$$

Finally, the constitutive equations are supplemented by:

The equation of conservation of linear momentum; Cauchy's dynamical equation of motion,

$$\rho \frac{D\underline{\upsilon}}{Dt} = \nabla \cdot \underline{\underline{\tau}} + \rho \underline{b}, \tag{35a}$$

in which "ρ" is the mass density and "b" the body force per unit mass and $\underline{\upsilon}$ is the velocity.

Continuity equation (for incompressible fluid);

$$\nabla \cdot \underline{\upsilon} = 0, \tag{35b}$$

Fiber equation of state;

$$\frac{D\underline{\underline{S}}_2}{Dt} = -\left(\underline{\underline{\omega}} \cdot \underline{\underline{S}}_2 - \underline{\underline{S}}_2 \cdot \underline{\underline{\omega}}\right) + \beta\left(\underline{\underline{\dot{\gamma}}} \cdot \underline{\underline{S}}_2 + \underline{\underline{S}}_2 \cdot \underline{\underline{\dot{\gamma}}} - 2\underline{\underline{\dot{\gamma}}} : \underline{\underline{S}}_4\right) + 2D_r\left(\underline{\underline{I}} - 3\underline{\underline{S}}_2\right). \tag{36}$$

In addition, we have to specify boundary conditions. Therefore, we assume for convenience the non-slip condition:

$$\underline{\upsilon} = \underline{0} \quad \text{on the boundary} \quad \Gamma, \tag{37a}$$

(no boundary condition is specified in respect of the orientation tensor) and the initial conditions:

$$\underline{\upsilon}(\underline{x}, 0) = \underline{\upsilon}_0, \qquad \underline{\underline{S}}_2(\underline{x}, 0) = \underline{\underline{S}}_2^0 \qquad \text{on } \Gamma. \tag{37b}$$

Examples of Constitutive Equations for Dilute Fiber Suspensions

Ericksen Equation

In the dilute range, the fluid behavior around each fiber is unaffected by the other. The medium is known to be governed by the Ericksen equation of state [47].

$$\underline{\underline{\tau}} = -P\underline{\underline{\delta}} + 2\mu_o \underline{\underline{\dot{\gamma}}} + \mu_2 \underline{\underline{\dot{\gamma}}}\,\underline{p}\,\underline{p}\,\underline{p}\,\underline{p}, \tag{38a}$$

where the rheological parameter μ_2, for a given aspect ratio a_r, is given by:

$$\mu_2 = \frac{a_r^2 \mu_o}{\ln a_r}. \tag{38b}$$

Lipscomb et al. Equation

Following Batchelor [48] and Evans [49], Lipscomb et al. [31] have proposed a model for dilute particle suspension, which can be written for ellipsoids with high aspect ratio as:

$$\underline{\underline{\tau}} = -P\underline{\underline{I}} + 2\mu_o \underline{\underline{\dot{\gamma}}} + \mu_o V_f\left(\mu_1 \underline{\underline{\dot{\gamma}}} + \mu_2 \underline{\underline{\dot{\gamma}}} : \underline{\underline{S}}_4\right), \tag{39}$$

The last term in equation 39 describes the coupling between hydrodynamic forces and fiber orientation, hence μ_2 is termed as the coupling coefficient. Lipscomb et al. [31] suggested that $\mu_1 = 2$ and $\mu_2 = \frac{a_r^2}{\ln a_r}$, and Evans [49, 50] further derived from the slender theory of Batchelor [51] to obtain $\mu_2 = \frac{8a_r^2}{3\ln a_r}$.

Examples of Constitutive Equations for Semi-Dilute Fiber Suspensions

In the semi-dilute range, the medium is submitted to two additional types of interactions namely, the "fiber-boundaries" and the "fiber-fiber" which affect the dynamics of the flow. These interactions appear either between the fiber and the boundaries or between neighboring fibers. The "fiber-boundaries" interactions are negligible with respect to the "fiber-fiber" interactions.

Batchelor Equation

A general constitutive equation for the bulk stress in a semi-dilute suspension containing cylindrical fibers was originally developed by Batchelor [51]. The equation can be expressed in the form of orientation stress tensors as follows:

$$\underline{\underline{\tau}} = \mu_o \dot{\underline{\underline{\gamma}}} + \tfrac{1}{2}\mu_p \left[\langle \underline{\underline{\underline{\underline{pppp}}}} \rangle - \tfrac{1}{3}\underline{\underline{\delta}} \langle \underline{\underline{pp}} \rangle \right] : \dot{\gamma}, \tag{40}$$

where $\mu_p = \frac{1}{6}\pi n L^3 \mu_o \varepsilon$ is the fiber extra viscosity and $\varepsilon = [\ln(2r_p)]^{-1}$.

Dinh-Armstrong Integral Model

The bulk stress in a suspension of particles in a Newtonian fluid obtained by Batchelor [51] has two separate parts, one due to the viscous dissipation of the fluid and the other due to the presence of particles. This model provides a direct link between the micro-structural properties and the macroscopic rheological behavior of a suspension system. Dinh et al. [46] applied this model to semi-concentrated fiber suspensions and obtained the rheological equation:

$$\underline{\underline{\tau}} = -\mu_o \dot{\underline{\underline{\gamma}}} \left\{ 1 + \frac{\pi}{12} \frac{(nL^3)}{\ln(2h/D)} : \int \underline{\underline{\underline{\underline{pppp}}}}\, \Psi(\underline{p}, t)\, d\underline{p} \right\}, \tag{41a}$$

with

$$\Psi(\underline{p}, t) = \frac{1}{4\pi} \left(\Delta^T \cdot \Delta : \underline{\underline{pp}} \right)^{-3/2} \tag{41b}$$

where Δ is the deformation gradient; $(\nabla \underline{V})^T$. When equation 41a is combined with equation 41b the constitutive equation for the fiber suspension is reduced to:

$$\underline{\underline{\tau}} = -\mu_o \dot{\underline{\underline{\gamma}}} \left\{ 1 + \frac{1}{48} \frac{nL^3}{\ln(2h/D)} : \int \frac{\underline{\underline{\underline{\underline{pppp}}}}\, d\underline{p}}{(\Delta^T \cdot \Delta : \underline{\underline{pp}})^{3/2}} \right\}. \tag{42a}$$

The product $[\Delta^T \cdot \Delta]$ appearing in equation 42a is known as the Cauchy strain tensor. It is sometimes convenient to use a finite strain tensor $\underline{\underline{\gamma}}^{[0]} = \left[\Delta^T \cdot \Delta - \underline{\underline{I}} \right]$ in terms of which equation 42a becomes:

$$\underline{\underline{\tau}} = -\mu_o \dot{\underline{\underline{\gamma}}} \left\{ 1 + \frac{1}{48} \frac{nL^3}{\ln(2h/D)} : \int \frac{\underline{\underline{\underline{\underline{pppp}}}}\, d\underline{p}}{(1 + \underline{\underline{\gamma}}^{[0]} : \underline{\underline{pp}})^{3/2}} \right\}. \tag{42b}$$

Equations (42a) and (42b) are similar in form in the way kinematical tensors appear to results obtained by Doi and Edwards [52] and Curtiss and Bird [53] for concentrated solutions of flexible macromolecules.

In the Dinh-Armstrong model and for cylinder bodies; the stress tensor in the dilute case is given as:

$$\underline{\underline{\tau}} = \mu_o \dot{\underline{\underline{\gamma}}} + \mu_o N \dot{\underline{\underline{\gamma}}} : \underline{\underline{\underline{S}}}_4, \tag{43}$$

where N is defined as a dimensionless suspension parameter which includes the combined effects of volume fraction V_f and fiber aspect ratio a_r.

The General Constitutive Equation

Finally, a general rheological constitutive equation for suspensions of axisymetric particles can be represented as follows [22]:

$$\tau_{ij} = \mu_o \dot{\gamma}_{ij} + \mu_o V_f \left[A \dot{\gamma}_{kl} a_{ijkl} + B(\dot{\gamma}_{ik} a_{kj} + a_{ik} \dot{\gamma}_{kj}) + C \dot{\gamma}_{ij} + 2F a_{ij} D_r \right] , \quad (44a)$$

where A, B, C and F are material constants which depend on the geometric shape factor. Various theories differ in the way which the constants A, B, C, and F are derived. For a slender particle, where thickness can be ignored, producing B and C equal to zero. If the particle is large enough so that Brownian motion can be ignored, the last term containing D_r can be omitted. Therefore, typical constitutive equation for fiber suspensions can be expressed as follows:

$$\tau_{ij} = \mu_o \dot{\gamma}_{ij} + \mu_o V_f \, A \dot{\gamma}_{kl} S_{ijkl} , \quad (44b)$$

APPENDIX

Simple Shear Flow

Simple shear flow will, as usual, be analyzed in a coordinate system where x_1 defines the flow direction, x_2 the direction of the flow gradient and x_3 the natural direction:

$$\nabla \underline{v} = \begin{bmatrix} 0 & 0 & 0 \\ \dot{\underline{\underline{\gamma}}} & 0 & 0 \\ 0 & 0 & 0 \end{bmatrix}, \quad \underline{\underline{D}} = \frac{1}{2} \begin{bmatrix} 0 & \dot{\underline{\underline{\gamma}}} & 0 \\ \dot{\underline{\underline{\gamma}}} & 0 & 0 \\ 0 & 0 & 0 \end{bmatrix}. \quad (A\text{-}1)$$

The rate of shear $\dot{\underline{\underline{\gamma}}}$ may also in general be understood as a function of time, but is a constant, say $\dot{\underline{\underline{\gamma}}}_{=o}$, in steady shear flow. For such flows, three rheological properties, namely the transient shear viscosity μ_o, first normal stress coefficient Ψ_1, and second normal stress coefficient Ψ_2, are of great importance. These rheological parameters are defined as:

$$\mu_o = \frac{\tau_{12}}{\left| \dot{\underline{\underline{\gamma}}} \right|}, \qquad \Psi_1 = \frac{\tau_{11} - \tau_{22}}{\left| \dot{\underline{\underline{\gamma}}} \right|^2}, \qquad \Psi_2 = -\frac{\tau_{22} - \tau_{33}}{\left| \dot{\underline{\underline{\gamma}}} \right|^2}, \quad (A\text{-}2)$$

where τ_{11}, τ_{22} and τ_{33} are the normal stresses and τ_{12} is the shear stress.

In the following, the solution of Jeffery's equation of motion for dilute fiber suspension; the exact formula, in simple shear flow is performed.

Analytical Solution of Orientation Tensors

Consider the motion of a rigid neutrally buoyant ellipsoidal particle in an arbitrary homogenous flow. The time rate of change of the orientation vector $\underline{p}(\theta, \varphi)$ of an ellipsoid of revolution can be expressed as:

$$\dot{p}_i = \left(\omega_{ij} + \alpha \dot{\gamma}_{ij} \right) p_j - \alpha p_i p_l p_k \dot{\gamma}_{kl} . \quad (A\text{-}3)$$

Following Bretherton's work [54], the solution of equation A-3 with the initial condition $p_i = p_i^o$; $t = t_o$ can shown to be,

$$p_i = \frac{E_{il} p_l^o}{\left(E_{lm} E_{lj} p_j^o p_m^o \right)^{1/2}} , \quad (A\text{-}4)$$

where E_{ij} are the components of the particle rotation tensor, defined by:

$$\frac{dE_{ij}}{dt} = \left(\omega_{ik} + \alpha \dot{\gamma}_{ik} \right) E_{kj} . \quad (A\text{-}5)$$

Equation (A-4), with the initial condition $\underline{\underline{E}} = \underline{\underline{I}}$ (unit tensor), provides the analytical solution of the rotation vector $\underline{p}(\theta, \varphi)$; and is valid for both two and three-dimensional flows and orientation fields. For infinite aspect ratio fibers (i.e., slender fibers) $\alpha = 1$ the rotation tensor E_{ij} becomes the actual strain tensor of the flow field and equation A-5 reduces to:

$$E_{ij} = \frac{\partial x_i}{\partial x_j^o} , \quad (A\text{-}6)$$

where x_i and x_j^o are the fluid particle coordinates at t and t^o ($t^o < t$), respectively. Hence, for $\alpha = 1$; E_{ij} is defined as the strain tensor for the undistorted flow.

In order to determine the particle rotation tensor components in terms of velocity gradients for planer orientations, two sets of differential equations, given by equation A-5, need to be solved with the initial condition $\underline{\underline{E}} = \underline{\underline{I}}$, [55]. Each set contains two coupled ordinary differential equations and can be solved independently. After obtaining analytical solutions of equation A-5, the orientation vector components can be easily calculated for any initial fiber orientation by using equation A-4.

For any two-dimensional homogenous flow, the velocity gradient tensor can be specified as:

$$u_{ij} = \begin{bmatrix} \frac{\partial u_1}{\partial x_1} & \frac{\partial u_1}{\partial x_2} \\ \frac{\partial u_2}{\partial x_1} & \frac{\partial u_2}{\partial x_2} \end{bmatrix} = \begin{bmatrix} c & c_1 \\ c_2 & -c \end{bmatrix}, \tag{A-7}$$

where c, c_1 and c_2 are arbitrary constants, and the trace of u_{ij} should be zero to satisfy the conservation of mass for incompressible flow. A single parameter w^2 can be utilized to define the solution families of equation A-7 with an arbitrary velocity gradient tensor.

$$w^2 = \frac{\alpha^2(B^2 + 4c^2) - A^2}{4}, \tag{A-8}$$

where $B = c_1 + c_2$ and $A = c_1 - c_2$. Depending on the value of w^2, three different solution families are possible as shown by Akbar and Altan [55].

When $w^2 = 0$,

$$E_{ij} = \begin{bmatrix} 1 + \alpha ct & \frac{(\alpha B + A)t}{2} \\ \frac{(\alpha B - A)t}{2} & 1 - \alpha ct \end{bmatrix}. \tag{A-9}$$

When $w^2 > 0$,

$$E_{ij} = \begin{bmatrix} \frac{w\cosh(wt) + \alpha c \sinh(wt)}{w} & \frac{(\alpha B + A)\sinh(wt)}{2w} \\ \frac{(\alpha B - A)\sinh(wt)}{2w} & \frac{w\cosh(wt) - \alpha c \sinh(wt)}{w} \end{bmatrix}. \tag{A-10}$$

When $w^2 < 0$,

$$E_{ij} = \begin{bmatrix} \frac{w\cos(wt) + \alpha c \sin(wt)}{w} & \frac{(\alpha B + A)\sin(wt)}{2w} \\ \frac{(\alpha B - A)\sin(wt)}{2w} & \frac{w\cos(wt) - \alpha c \sin(wt)}{w} \end{bmatrix}. \tag{A-11}$$

In equation A-10 w is defined as $w = \sqrt{|w^2|}$. Equations (A-9) – (A-11) are the possible solutions for particle rotation tensor and can be used in equation A-4 to specify the rotation of both oblate and prolate spheroids subjected to an arbitrary homogenous flow.

If the initial distribution of particle orientation is known, the time-dependent evolution of orientation distribution function can be obtained analytically. For planer orientations, using normalization condition as given in equation 8b, the initial condition for randomly oriented particles becomes:

$$\Psi(\underline{p}, t = 0) = \frac{1}{\pi}. \tag{A-12}$$

Therefore, for random initial condition, the solution of the Fokker-Planck equation; equation 14 with equation A-3 can be expressed as;

$$\Psi(\underline{p}, t) = \frac{1}{\pi}\left(\Lambda_{lm}\Lambda_{lj}p_j p_m\right)^{-1}, \tag{A-13}$$

where Λ_{ij} is the inverse of particle rotation tensor E_{ij}. Equation (A-13) can be rearranged by using planer orientation angle φ as;

$$\Psi(\varphi, t) = \frac{1}{\pi}\left(a_1\cos^2\varphi + \tfrac{1}{2}a_2\sin 2\varphi + a_3\sin^2\varphi\right)^{-1}, \tag{A-14}$$

where

$$a_1 = \Lambda_{11}^2 + \Lambda_{21}^2,$$
$$a_2 = 2(\Lambda_{11}\Lambda_{12} + \Lambda_{21}\Lambda_{22}),$$
$$a_3 = \Lambda_{12}^2 + \Lambda_{22}^2. \quad \text{(A-15)}$$

Determining analytical solutions of the second- and fourth-order orientation tensors involves calculation of the integrals given by equations 9a and 9b. For the second-order orientation tensor S_{ij}, the resulting integral becomes:

$$S_{ij} = \frac{1}{\pi}\int_0^{\pi} \frac{\cos^{(4-\zeta)}\varphi \sin^{(\zeta-2)}\varphi}{a_1\cos^2\varphi + \frac{1}{2}a_2\sin 2\varphi + a_3\sin^2\varphi}\,d\varphi \quad , \quad \text{(A-16)}$$

where $\zeta = i + j$. Similarly, the fourth-order orientation tensor S_{ijkl} can be expressed as:

$$S_{ijkl} = \frac{1}{\pi}\int_0^{\pi} \frac{\cos^{(8-\zeta)}\varphi \sin^{(\zeta-4)}\varphi}{a_1\cos^2\varphi + \frac{1}{2}a_2\sin 2\varphi + a_3\sin^2\varphi}\,d\varphi, \quad \text{(A-17)}$$

where $\zeta = i + j + k + l$. Consequently, the S_{ij} components are obtained as:

$$S_{11} = \frac{1}{2\Delta_1}\left[a_2^2 - 2(a_3 - a_1)(1 - a_3)\right], \quad \text{(A-18)}$$

$$S_{12} = \frac{1}{2\Delta_1}\left[2a_2 - a_2(a_1 - a_3)\right], \quad \text{(A-19)}$$

$$S_{22} = \frac{1}{2\Delta_1}\left[a_2^2 + 2(a_3 - a_1)(1 - a_1)\right], \quad \text{(A-20)}$$

From equation A-17, the S_{ijkl} components becomes:

$$S_{1111} = \frac{(a_1 - 3a_3)[(a_1 - a_3)^2 - a_2^2] + 4a_2^2(a_1 - a_3)}{2\Delta_1^2} + \frac{2a_3^4 + 2a_3^2a_2^2 + a_2^4 - 4a_1a_3^3 - 4a_1a_2^2a_3 + 2a_1^2a_3^2}{\Delta_1^2\Delta_2}, \quad \text{(A-21)}$$

$$S_{1112} = -\frac{4a_3a_2(a_1 - a_3) + a_2[(a_1 - a_3)^2 - a_2^2]}{2\Delta_1^2} + \frac{a_2(3a_1^2a_3 - a_1a_2^2 - 2a_1a_3^2 - a_3^3)}{\Delta_1^2\Delta_2}, \quad \text{(A-22)}$$

$$S_{1122} = \frac{(a_1 + a_3)[(a_1 - a_3)^2 - a_2^2]}{2\Delta_1^2} + \frac{a_3^2a_2^2 - 2a_1a_3^3 + 4a_1^2a_3^2 + a_1^2a_2^2 - 2a_1^3a_3}{\Delta_1^2\Delta_2}, \quad \text{(A-23)}$$

$$S_{1222} = \frac{a_2[-(a_1 - a_3)^2 + a_2^2] + 4a_1a_2(a_1 - a_3)}{2\Delta_1^2} + \frac{a_2[3a_1a_3^2 - a_1^3 - 2a_1^2a_3 - a_2^2a_3]}{\Delta_1^2\Delta_2}, \quad \text{(A-24)}$$

$$S_{2222} = \frac{(a_3 - 3a_1)[(a_1 - a_3)^2 - a_2^2] - 4a_2^2(a_1 - a_3)}{2\Delta_1^2} + \frac{a_2^4 - 4a_1a_2^2a_3 + 2a_1^2a_2^2 + 2a_1^2a_3^2 + 2a_1^4 - 4a_1^3a_3}{\Delta_1^2\Delta_2}. \quad \text{(A-25)}$$

where $\Delta_1 = (a_1 - a_3)^2 + a_2^2$ and $\Delta_2 = \sqrt{4a_1a_3 - a_2^2}$.

Second and Fourth Order Tensor Components of Simple Shear Flow

The velocity gradient tensor for a simple shear flow is expressed as:

$$u_{ij} = \begin{bmatrix} 0 & c_1 \\ 0 & 0 \end{bmatrix}, \quad \text{(A-26)}$$

where c_1 represents the shear rate. It can be easily seen that w^2, defined in equation A-8, becomes

$$w^2 = \frac{c_1^2(\alpha^2 - 1)}{4}. \quad \text{(A-27)}$$

Since $\alpha^2 < 1$ for finite aspect ratio particles, $w^2 < 0$. Therefore, the second- and fourth-order orientation tensor components for the simple shear flow simplify as:

$$S_{11} = \Delta_3\left(b_1 + b_1 b_3 - b_3 + b_3^2 - 2\right), \quad \text{(A-28)}$$

$$S_{12} = \frac{1}{2}\Delta_3 b_2 (2 - b_1 - b_3), \quad \text{(A-29)}$$

$$S_{22} = \frac{1}{2}\Delta_3\left(b_1^2 - b_1 + b_1 b_3 + b_3 - 2\right), \quad \text{(A-30)}$$

$$S_{1111} = \frac{1}{2}\Delta_3^2 (b_1 + b_3 - 2)^2 (4 + b_1 + 5b_3 + 2b_3^2), \quad \text{(A-31)}$$

$$S_{1112} = -\frac{1}{2}\Delta_3^2 b_2 (b_1 + b_3 - 2)^2 (1 + b_3), \quad \text{(A-32)}$$

$$S_{1122} = \frac{1}{2}\Delta_3^2 (b_1 + b_3 - 2)^2 (b_1 + 2b_1 b_3 + b_3), \quad \text{(A-33)}$$

$$S_{1222} = -\frac{1}{2}\Delta_3^2 b_2 (b_1 + b_3 - 2)^2 (1 + b_3), \quad \text{(A-34)}$$

$$S_{2222} = \frac{1}{2}\Delta_3^2 (b_1 + b_3 - 2)^2 (4 + 2b_1^2 + 5b_1 + b_3), \quad \text{(A-35)}$$

where

$$\Delta_3 = \left[(b_1 + b_3)^2 - 4\right]^{-1}, \quad \text{(A-36)}$$

$$b_1 = 1 - \frac{2\alpha}{1+\alpha}\sin^2 wt, \quad \text{(A-37)}$$

$$b_2 = -\frac{2\alpha}{\sqrt{1+\alpha^2}}\sin 2wt, \quad \text{(A-38)}$$

$$b_3 = 1 + \frac{2\alpha}{1-\alpha}\sin^2 wt, \quad \text{(A-39)}$$

REFERENCES

[1] Park, J.M. and Park, S.J. 2011. Modeling and simulation of fiber orientation in injection molding of polymer composites. Mathematical problems in physics.

[2] Duang-Hong, D., Thien, N.P., Yeo, K.S. and Ausias, G. 2010. Dissipative particle dynamics simulations for fiber suspensions in Newtonian and viscoelastic fluids. Computer Methods in applied mechanics and engineering. 199, Issues 23-24, 1593-1602.

[3] Einstein, A. 1906. Eine neue bestimmung der molekuldimensionen. Ann. Physik, 19, 289-306.

[4] Jeffery, G.B. 1922. The motion of ellipsoidal particles immersed in a viscous fluid. Proc. R. Soc. London, A 102(715), 161-179.

[5] Leal, L.G. and Hinch, E.J. 1971. The effect of weak Brownian rotations on particles in shear flow. J. Fluid Mech. 46, 685.

[6] Leal, L.G. and Hinch, E.J. 1972. The rheology of a suspension of nearly spherical particles subject to Brownian rotations. J. Fluid Mech. 55, 745.

[7] Hinch, E.J. and Leal, L.G. 1975. Constitutive equations in suspension mechanics. Part I. General formation. J. Fluid Mech. 71(3), 481-495.

[8] Hinch, E.J. and Leal, L.G. 1976. Constitutive equations in suspension mechanics. Part II. Approximate forms for a suspension of rigid particles affected by Brownian rotations. J. Fluid Mech. 76(1), 187-208.

[9] Hinch, E.J. and Leal, L.G. 1972. The effect of Brownian motion on the rheological properties of a suspension on non-spherical particles. J. Fluid Mech. 52, 683.

[10] Leal, L.G. and Hinch, E.J. 1973. Theoretical studies of a suspension of rigid particles affected by Brownian couples. Rheol. Acta, 12, 127.

[11] Hinch, E.J. and Leal, L.G. 1973. Time-dependent shear flows of a suspensions of particles with weak Brownian rotations. J. Fluid Mech. 57, 753.

[12] Batchelor, G.K. 1970. The stress system in a suspension of force-free particles. J. Fluid Mech. 41(3), 545-570.

[13] Pabst, W. 2004. Fundamental considerations on suspension rheology. Ceramics-Silikaty 48 (1), 6-13.

[14] Rodriguez, F. 1983. Principles of polymer systems. 2nd edition McGraw-Hill chemical engineering series.

[15] Hand, G.L. 1961. A theory of dilute suspensions. Arch. Ration. Mech. Anal., 7, 81-86.

[16] Crowe, C. 1982. Review-numerical models for dilute gas-particles flow. J. Fluids Eng., Tran. ASME 104, 297.

[17] Doi, M. and Edwards, S. 1978. Dynamics of rod-like macromolecules in concentrated solution. I. J. Chem. Soc. Faraday Trans. II, 74, 560.

[18] Doi, M. 1981. Molecular dynamics and rheological properties of concentrated solutions of rodlike polymers in isotropic and liquid crystalline phases. J. Polym. Sci. Part B Polym. Phys. Ed., 19, 229-243.

[19] Pipes, R.B., Mc Cullough, R.L. and Taggart, D.G. 1982. Behavior of discontinuous fiber composites: fiber orientation. Polym. Composites, 3(1), 34-39.

[20] Agari, Y., Ueda, A. and Nagai, S. 1991. Thermal conductivity of polyethylene filled with disoriented short-cut carbon fibers. J. Appl. Polym. Sci., 43 (6), 1117-1124.

[21] Eberle, A.P.R. and Baird, D.G. 2009. Using transient shear rheology to determine material parameters in fiber suspension theory. J. Rheol. 53(3), 685-705.

[22] Massoudi, M. 2005. An anisotropic constitutive relation for the stress tensor of a rod-like (fibrous-type) granular material. Mathematical problem in engineering 6, 679-702.

[23] Pipkin, 1972. Lectucres on viscoelasticity theory. Springer-Verlag New York-Heidelberg-Berlin, (1972).

[24] Pabst, W. and Gregorova, E. 2003. Effective elastic properties of Alumina-Zirconia composite ceramics – part 1. Rational continuum theory of linear elasticity. Ceramics – Silikaty, 47, 1-7.

[25] Atankovic, T.M. 2000. Theory of elasticity for scientists and engineers. Birkhauser, Boston.

[26] Cintra, J.S. and Tucker III, C.L. 1995. Orthotropic closure approximations for flow-induced fiber orientation. J. Rheol. 39 (6), 1095-1122.

[27] Atankovic, T.M. 2000. Theory of elasticity for scientists and engineers. Birkhauser, Boston.

[28] Advani, S.G. and Sozer, E.M. 2003. Process modeling in composites manufacturing. Marcel Dekker Inc., New York.

[29] Advani, S.G. and Tucker III, C.L. 1990. Closure approximations for three-dimensional structure tensors. J. Rheol. 34(3), 367-386.

[30] Hand, G.L., 1961. A theory of dilute suspensions. Arch. Ration. Mech. Anal. 7, 81-86.

[31] Lipscomb, G.G., Denn, M.M., Hur, D.U. and Boger, D.V. 1988. The flow of fiber suspensions in complex geometries. J. Non-Newtonian Fluid Mech., 26, 297-325.

[32] Arrhenius, S., Z. Physik. Chem. 1, 285 (1887).

[33] Advani, S.G. and Tucker, C.L. 1987. The use of tensors to describe and predict fiber orientation in short fiber composites. J. Rheol. 31(8), 751-784.

[34] Folgar, F. and Tucker III, C.L. 1984. Orientation behavior of fibers in concentrated suspensions. J. Reinforced Plastics and Composites, 3(2), 98-119.

[35] Bay, B.S. 1991. Fiber orientation in injection molded composites: A comparison of theory and experiment, PhD thesis, Mech. Eng., Univ. of Illinois at Urbana-Champaign.

[36] Phan-Thien, N., Fan, X.J., Tanner, R.I. and Zheng, R. 2002. Folgar-Tucker constant for a fiber suspension in a Newtonian fluid. J. Non-Newtonian Fluid Mech., 103, 251-260.

[37] Sepehr, M., Ausias, G. and Carreau, P.J. 2004. Rheological properties of short fiber filled polypropylene in transient shear flow. J. Non-Newtonian Fluid Mech. 123: 19-32.

[38] Chung, D.H. and Kwon, T.H. 2002. Invariant-based optimal fitting closure approximation for the numerical prediction of flow-induced fiber orientation. J. Rheol. 46(1), 169-194.

[39] Han, K.H. and Im, Y.T. 1999. Modified hybrid closure approximation for prediction of flow-induced fiber orientation. J. Rheol. 43(3), 569-589.

[40] Chung, D.H. and Kwon, T.H. 1998. Improved closure approximation for numerical simulation of fiber orientation in fiber-reinforced composite. The Korean J. Rheol. 10(4), 202-216.

[41] Chung, D.H. and Kwon, T.H. 2001. Improved model of orthotropic closure approximation for flow induced fiber orientation. Polymer composites, 22(5), 636-649.

[42] Chung, D.H. and Kwon, T.H. 2002a. Invariant-based optimal fitting closure approximation for the numerical prediction of flow-induced fiber orientation. J. Rheol. 46(1), 169-194.

[43] Hand, G.L. 1962. A theory of anisotropic fluids. J. Fluid Mech. 13, 33-62.

[44] Jack, D.A., Schache, B. and Smith, D.E. 2010. Neural network-based closure for modeling short-fiber suspensions. Polymer Composites, 31(7), 1125-1141.

[45] Shaqfeh, E.S.G. and Fredrickson, G.H. 1990. The hydrodynamic stress in a suspension of rods. Phys. Fluids, A, 2(1) 7-24.

[46] Dinh, S.M. and Armstrong, R.C. 1984. A rheological equation of state for semi-concentrated fiber suspensions. J. Rheol. 28(3), 207-227.

[47] Ericksen, J.L. 1960. Transversely isotropic fluids. Kollid-Z., 173, 117-122.

[48] Batchelor, G.K. 1970. The stress system in a suspension of force-free particles. J. Fluid Mech. 41(3), 545-570.

[49] Evans, J.G. 1975. The flow of a suspension of force-free rigid rods in a Newtonian fluids. PH.D. dissertation University of Cambridge.

[50] Evans, J.G. 1975. The effect of Non-Newtonian properties of a suspension of rod –like particles on flow fields. in: J.R.A. Pearson, K. Walter, J.F. Hutton (Eds), Theoretical Rheology, Halstead Press, New York.

[51] Batchelor, G.K. 1971. The stress generated in a non-dilute suspension of elongated particles by pure straining motion [J]. J. Fluid Mech. 46(4), 813-829.

[52] Doi, M. and Edwards, S.F. 1979. Dynamics of rod-like macromolecules in concentrated solution. J. Chem. Soc. Faraday Trans. 2. 74, 1789, 1802, 1818 (1978); 75, 38.

[53] Curtiss C.F., Bird, R.B. 1981. J. Chem. Phys., 74, 2016-2026.

[54] Bretherton's, F.P. 1962. The motion of rigid particles in a shear flow at low Reynolds Number. J. Fluid Mech. 14, 284-304.

[55] Akbar, S. and Altan, M.C. 1992. On the solution of fiber orientation in two dimensional homogenous flows. Polym. Eng. Sci., 32 (12), 810-822.